Stability Considerations for Variable Impedance Control

Klas Kronander and Aude Billard

***Abstract*—Impedance control is a commonly used control architecture for robotic manipulation. For increased flexibility, the impedance can be programmed to vary during the task. This has important implications on the stability properties of the control system, which are often overlooked in practice. In fact, the standard stability analysis is not valid in the case that the impedance parameters vary over time. Simulations show that, depending on how the impedance parameters are varied, stable or unstable behavior can arise even in regulation without contact. In this paper, we elucidate this issue and propose a state-independent stability constraint that relates the stiffness, and also the time derivative of the stiffness to the damping. Our approach is illustrated and evaluated in comparison with an online stabilization method [8] which uses a tank-based stability criterion.**

***Index Terms*—Manipulator dynamics, robot control, stability criteria.**

I. Introduction

Impedance control [11] is a suitable control architecture to improve the performance of robotic manipulation in many situations in which traditional control paradigms are prone to failure. Examples include tasks with uncertain pose estimates of manipulated objects, physical contact and tasks in which it is important to respond appropriately to unforeseen perturbations [28]. Recently, many researchers have explored the benefit of varying the impedance during the task [4], [5], [17], [18], [29]. Variable impedance control allows not only controlling the dynamic relationship between external forces and robot movements, but in addition gives the flexibility to change these dynamics in a continuous manner during the task.

Variable impedance control requires more complex task models than position-controlled or fixed impedance-controlled systems, as the impedance profile must be represented in addition to position (and possibly force) information. Several works have addressed the problem of the specification of varying impedance through geometrical task information [20], optimal control [3], [9], [21], learning by demonstration [5], [18], reinforcement learning [4], [17], [23], and imitation of human impedance [1], [13]. These works have demonstrated the usefulness of variable impedance control, and suggested several different methods for defining or learning impedance profiles for tasks. However, none of these works address the issue of guaranteeing stable execution of learned tasks with variable impedance.

Manuscript received March 27, 2015; revised November 16, 2015 and June 21, 2016; accepted July 5, 2016. Date of publication September 5, 2016; date of current version September 30, 2016. This paper was recommended for publication by Associate Editor S. Kim and Editor T. Murphey upon evaluation of the reviewers' comments. This work was supported by the European FP7 project RoboHow (FP7-ICT-288533).

The authors are with the Learning Algorithms and Systems Laboratory, Swiss Federal Institute of Technology, Lausanne 1015, Switzerland, (e-mail: klas.kronander@epfl.ch; aude.billard@epfl.ch).

Color versions of one or more of the figures in this paper are available online at http://ieeexplore.ieee.org.

Digital Object Identifier 10.1109/TRO.2016.2593492

Impedance control can be realized in joint, Cartesian, or other task-specific coordinates. The impedance objective can be achieved in different ways, e.g., actively on torque-controlled backdrivable manipulators or passively through placement of elastic elements between the actuators and the joints [2], [10], [22]. With constant gains, impedance control makes the closed-loop system passive and hence passive (and stable) in interaction with passive environments [7], [12]. However, the passivity property is lost if arbitrary variations of the impedance parameters are allowed.

Adaptive control is a powerful means of adapting unknown model parameters for feed-forward controllers [27]. There are also adaptive controllers that result in varying feedback gains, and design the adaptation laws of the feedback gains so as to prove stability [29]. Adaptive control has also been used to improve force tracking in impedance control with stability guarantee [14]. Such adaptation laws then generate a variable impedance profile online as a result of how the task unfolds. Unlike the adaptive control approach, which uses adaptation rules to vary the gains to achieve stability, our work is concerned with the analysis of variable impedance profiles that already exist prior to task execution.

As in variable impedance control, varying feedback gains arise in gain scheduling control design. Gain scheduling is a family of control design techniques aimed at applying linear controller design to nonlinear systems. The process starts by deriving local linearizations around certain operating points of interest. Then, linear controllers with fixed gains are designed for each of these linearizations. Finally, the controller is achieved by interpolating these feedback gains as the system transitions between the operating points, resulting in varying feedback gains [24]. Gain scheduling relies on applying rules-of-thumb such as slow parameter variations, and extensive simulation is required to investigate the global stability and performance of the closed-loop system. Even though there are methods that quantify "slow variations" in certain cases [25], these results do not apply to our case. In contrast to gain scheduling, which is concerned with finding gain schedules to achieve certain criteria in nonlinear control problems, we address the problem of guaranteeing the stability of an already existing trajectory of varying feedback gains. Our problem setting hence is different, since we start with a desired variable impedance and want to verify that it can be executed without losing stability.

There is hence a need for analysis or control methods that can guarantee stable execution of variable impedance tasks. This issue has been recently addressed in [8], wherein a tank-based approach to passive varying stiffness was proposed. Their system uses the total energy of the manipulator (kinetic plus virtual potential energy coming from stiffness term), but does not constrain this function to strictly decrease. Instead, any dissipated

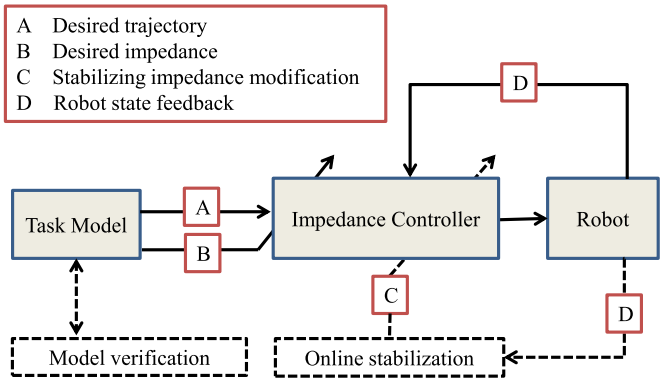

Fig. 1. Block diagram illustrating two different approaches to guarantee stability of varying impedance systems. The method proposed in this paper consists of a state-independent task model verification that can be carried out offline. The alternative approach involves online computation of an energy function and limitation of the impedance variations so as to ensure monotonic decline.

energy is added to a virtual energy tank, from which energy can be extracted in order to implement stiffness variations. The tank is given an initial level of energy and a maximum allowed level of energy. These levels determine to what extent the system will accept stiffness variations. This is an elegant approach based on a sound energy-based idea. However, it has two important shortcomings, which are as follows.

1) It depends on the state of the robot, with the consequence that one cannot guarantee beforehand the execution of a desired impedance profile.
2) The performance depends strongly on the intial and threshold levels of energy in the tank.[1]

Our aim with this work is to provide a stability condition for varying stiffness and damping that is *state independent*. The most important practical advantage of such a constraint is that it can be verified offline, before execution of the task. Any standard impedance control architecture can subsequently be used for task execution, with a reassuring guarantee that the system cannot go unstable. The two different approaches are illustrated in Fig. 1.

We focus on variable stiffness and damping, which are the impedance parameters that are most commonly varied for improving task performance. We then propose a stability condition that relates the stiffness, damping, and their rates of change. The constraint arises from the choice of a Lyapunov candidate function in which mixed position and velocity terms appear in the time derivative. Our main contribution in this paper is using this function to derive stability constraints for stiffness and damping profiles, and evaluating how these constraints can be used in practice.

This paper is structured as follows. Section II contains a presentation of the impedance controller used in this paper, and the stability analysis for the fixed gain case. In Section III, we present our main result, a stability constraint for variable stiffness and damping control. The method is compared with the state-of-the-art tank-based method [8] through two task simulations in Section IV-A. We then use our result to validate real impedance profiles in Section IV-B. We conclude with a discussion and outlook into future directions of research in Section V.

[1]For example, practically unstable behavior can emerge by setting the levels to be very high.

II. Preliminaries

The technical presentation and stability analysis will be done in joint space in this paper. The controllers in this section as well as our algorithms in Section III can equivalently be expressed in Cartesian coordinates, using the operational space dynamic equations [16].

A. Rigid Body Dynamics

We assume that the physics of the manipulator is accurately described by the rigid-body form as

$$\mathbf{M}(\mathbf{q})\ddot{\mathbf{q}} + \mathbf{C}(\dot{\mathbf{q}}, \mathbf{q})\dot{\mathbf{q}} + \mathbf{g}(\mathbf{q}) = \boldsymbol{\tau}_c + \boldsymbol{\tau}_e \tag{1}$$

where $\mathbf{q}, \dot{\mathbf{q}}, \ddot{\mathbf{q}} \in \mathbb{R}^N$ denote the position, velocity, and acceleration of N joints of the robot, $\mathbf{M}(\mathbf{q}) \in \mathbb{R}^{N\times N}$ the symmetric and positive definite joint space inertia matrix, $\mathbf{C}(\dot{\mathbf{q}}, \mathbf{q}) \in \mathbb{R}^{N\times N}$ the Coriolis/centrifugal matrix, and $\mathbf{g}(\mathbf{q}) \in \mathbb{R}^N$ the torque due to gravity. The control torques and external torques are denoted by $\boldsymbol{\tau}_c \in \mathbb{R}^N$ and $\boldsymbol{\tau}_e \in \mathbb{R}^N$, respectively.

B. Impedance Control

In joint space impedance control, the objective is to maintain the following dynamic relationship between external torque $\boldsymbol{\tau}_e$ and position error $\tilde{\mathbf{q}}$:

$$\mathbf{H}\ddot{\tilde{\mathbf{q}}} + \mathbf{D}\dot{\tilde{\mathbf{q}}} + \mathbf{K}\tilde{\mathbf{q}} = \boldsymbol{\tau}_e \tag{2}$$

where $\mathbf{H} \in \mathbb{R}^{N\times N}$, $\mathbf{D} \in \mathbb{R}^{N\times N}$, and $\mathbf{K} \in \mathbb{R}^{N\times N}$ denote a desired inertia, damping, and stiffness respectively. $\mathbf{H}, \mathbf{D}$, and $\mathbf{K}$ are positive definite and $\mathbf{H}, \mathbf{K}$ are symmetric. Let $\{\ddot{\mathbf{q}}_t^r, \dot{\mathbf{q}}_t^r, \mathbf{q}_t^r\}_{t=0}^T$ be a given reference trajectory, and let $\boldsymbol{\tau}_c$ be an inverse dynamics command

$$\boldsymbol{\tau}_c = \mathbf{M}(\mathbf{q})\boldsymbol{\nu} + \mathbf{C}(\dot{\mathbf{q}}, \mathbf{q})\dot{\mathbf{q}} + \mathbf{g}(\mathbf{q}) - \boldsymbol{\tau}_e. \tag{3}$$

Define the new control input $\boldsymbol{\nu}$ as

$$\boldsymbol{\nu} = \ddot{\mathbf{q}}_t^r + \mathbf{H}^{-1}(-\mathbf{D}(\dot{\mathbf{q}} - \dot{\mathbf{q}}_t^r) - \mathbf{K}(\mathbf{q} - \dot{\mathbf{q}}_t^r) + \boldsymbol{\tau}_e). \tag{4}$$

Substituting (3) and (4) in (1) and introducing the notation $\tilde{\mathbf{q}} = \mathbf{q} - \mathbf{q}_t^r$ yields the closed-loop dynamics in (2).

The user-defined virtual inertia $\mathbf{H}$, damping $\mathbf{D}$, and stiffness $\mathbf{K}$ determine the behavior of the robot when subjected to external torque. If these parameters are constant, the system will be asymptotically stable for any symmetric positive definite choice of matrices $\mathbf{H}$, $\mathbf{D}$, and $\mathbf{K}$. In this work, we are concerned with varying impedance control. Specifically, we will assume that $\mathbf{H}$ remains constant while $\mathbf{D}(t)$ and $\mathbf{K}(t)$ are considered time-varying functions. Note that in order to implement such an impedance controller, measurement of external effort (e.g., via joint torque sensors) is required.

C. Stability Analysis

To analyze the stability properties of (2), consider the following Lyapunov candidate function:

$$V_1(\tilde{\mathbf{q}}, \dot{\tilde{\mathbf{q}}}, t) = \frac{1}{2}\dot{\tilde{\mathbf{q}}}^T \mathbf{H}\dot{\tilde{\mathbf{q}}} + \frac{1}{2}\tilde{\mathbf{q}}^T \mathbf{K}(t)\tilde{\mathbf{q}}. \tag{5}$$

For compactness of notation, we will refer to $V_1(\dot{\tilde{\mathbf{q}}}, \tilde{\mathbf{q}}, t)$ as simply V_1 in the remainder of this paper. Differentiating V_1 along the trajectories of (2) with $\boldsymbol{\tau}_e = 0$ and $\mathbf{H}$ constant yields

$$\begin{aligned}\dot{V}_1 &= \dot{\tilde{\mathbf{q}}}\mathbf{H}\ddot{\tilde{\mathbf{q}}} + \tilde{\mathbf{q}}^T \mathbf{K}(t)\dot{\tilde{\mathbf{q}}} + \frac{1}{2}\tilde{\mathbf{q}}^T \dot{\mathbf{K}}(t)\tilde{\mathbf{q}} \\ &= \dot{\tilde{\mathbf{q}}}^T(-\mathbf{D}(t)\dot{\tilde{\mathbf{q}}} - \mathbf{K}(t)\tilde{\mathbf{q}}) + \dot{\tilde{\mathbf{q}}}^T \mathbf{K}(t)\tilde{\mathbf{q}} + \frac{1}{2}\tilde{\mathbf{q}}^T \dot{\mathbf{K}}(t)\tilde{\mathbf{q}}\end{aligned}$$

where symmetry of the stiffness matrix has been used. The mixed term with $\dot{\tilde{\mathbf{q}}}$ and $\tilde{\mathbf{q}}$ is hence cancelled but the potentially positive term with $\dot{\mathbf{K}}$ remains

$$\dot{V}_1 = -\dot{\tilde{\mathbf{q}}}^T \mathbf{D}(t)\dot{\tilde{\mathbf{q}}} + \frac{1}{2}\tilde{\mathbf{q}}^T \dot{\mathbf{K}}(t)\tilde{\mathbf{q}}. \tag{6}$$

Equation (6) is negative semidefinite for a negative semidefinite $\dot{\mathbf{K}}(t)$. Hence, we can conclude stability at the origin only if all the eigenvalues of the stiffness matrix are either constant or decreasing. Assuming $\tilde{\mathbf{q}} \neq 0$, increasing the stiffness eigenvalues can inject potential energy into the system, and it is hence intuitively clear that this practice can cause unstable behavior.

III. Ensuring Stability

As seen from (6), the classical energy function does not allow us to conclude stability with a varying stiffness profile. By inspection of the expression in (6), the obvious solution to the problem would be to design a controller that tries to follow the desired stiffness profile as well as possible, but limiting it when (6) becomes positive. However, such an approach has several disadvantages, the most important being 1) the admissible stiffness profile *depends on the state of the robot* and can hence not be known beforehand and 2) there are no guarantees in terms of capability of following the desired stiffness profile. By introducing the concept of an energy tank as in [8], the second of these drawbacks can be somewhat relaxed.

A. Stability Conditions on Stiffness and Damping Profiles

Experience of varying stiffness control suggests that in general, reasonable varying stiffness profiles show no destabilization tendencies. This motivates the search for a less conservative Lyapunov candidate function than (5). In adaptive control, it is common to construct energy functions of weighted sums of the velocity error and the position error. The same approach can be used for varying stiffness control to establish state-independent stability conditions relating the stiffness and damping profiles. Consider the following Lyapunov candidate function:

$$V_2(\tilde{\mathbf{q}}, \dot{\tilde{\mathbf{q}}}, t) = \frac{(\dot{\tilde{\mathbf{q}}} + \alpha\tilde{\mathbf{q}})^T \mathbf{H}(\dot{\tilde{\mathbf{q}}} + \alpha\tilde{\mathbf{q}})}{2} + \frac{\tilde{\mathbf{q}}^T \boldsymbol{\beta}(t)\tilde{\mathbf{q}}}{2} \tag{7}$$

where

$$\boldsymbol{\beta}(t) = \mathbf{K}(t) + \alpha\mathbf{D}(t) - \alpha^2\mathbf{H} \tag{8}$$

with some positive constant α chosen, such that $\boldsymbol{\beta}(t)$ is positive semidefinite for all $t > 0$. This candidate function is a generalized version of a Lyapunov function which is used for the analysis of time-varying scalar systems in [26]. Note that $\alpha \to 0 \Rightarrow V_2 \to V_1$. In contrast to V_1, however, this function allows to establish sufficient constraints for stability that are *independent of the state*. This is formalized in the following theorem.

Theorem 1 (Stability Conditions Under Dynamic Decoupling): Let $\mathbf{H}$ be a constant, symmetric, and positive definite matrix. Let $\mathbf{K}(t)$ and $\mathbf{D}(t)$ be symmetric, positive definite, and continuously differentiable varying stiffness and damping profiles. Then, the system in (2) with $\boldsymbol{\tau}_e = \mathbf{0}$ is globally uniformly stable if there exists an $\alpha > 0$, such that $\forall\, t \geq 0$:

1) $\alpha\mathbf{H} - \mathbf{D}(t)$ is negative semidefinite
2) $\dot{\mathbf{K}}(t) + \alpha\dot{\mathbf{D}}(t) - 2\alpha\mathbf{K}(t)$ is negative semidefinite

If in (2) semidefiniteness is replaced with definiteness, the stability property is in addition asymptotic.

Proof: The proof is given in Appendix B ■

It is perhaps not intuitively clear why the derivative of the damping appears in the second condition of Theorem 1. In the analysis in Section II-B, $\dot{\mathbf{D}}$ does not appear in $\dot{V}_1$ (6). This means that for a constant stiffness, stability would be ensured by any positive definite $\mathbf{D}$, without any direct constraints[2] on $\dot{\mathbf{D}}$. Increasing the damping too fast, however, can make the system converge at points with $\dot{\tilde{\mathbf{q}}} = 0$ but $\tilde{\mathbf{q}} \neq 0$ [26] and hence compromise asymptotic stability. The presence of $\dot{\mathbf{D}}$ in second condition in Theorem 1 prevents this from happening, since both $\dot{\mathbf{K}}$ and $\dot{\mathbf{D}}$ are in effect bounded by this constraint. Note that for robotic applications, this condition will typically be simplified to a form that has a more intuitive interpretation. We illustrate this point with two examples below, with a scalar system given by

$$m\ddot{q} + d(t)\dot{q} + k(t)q = 0. \tag{9}$$

Example 1 (Constant damping): Consider the system in (9) with constant damping $d(t) = d_0 > 0$, implying $\dot{d}(t) = 0$. The stability conditions from Theorem 1 then reduce to

$$d_0 > \alpha m \tag{9a}$$

$$\dot{k}(t) < 2\alpha k(t). \tag{9b}$$

Here, the second condition is an upper bound for the stiffness derivative that is proportional to the current stiffness and the minimum level of damping (as a multiple of the system mass).

Example 2 (Constant damping ratio): Consider the system in (9) with the damping chosen as $d(t) = 2\zeta\sqrt{mk(t)}$, where $\zeta > 0$ is a constant damping ratio.

Substituting $\dot{d}(t) = \frac{2\zeta\sqrt{m}}{\sqrt{k(t)}}\dot{k}(t)$ into the second condition yields the following upper bound for the stiffness time-derivative:

$$\dot{k}(t) < \frac{2\alpha\sqrt{k(t)}^3}{\sqrt{k(t)} + 2\zeta\alpha\sqrt{m}}. \tag{10}$$

[2]There are constraints that follow from positive definiteness of $\mathbf{D}$.

B. Validating Impedance Profiles

The stability conditions presented in the previous section are constraints only on the stiffness and damping profiles. This means that it can be directly incorporated in an optimization or learning procedure, which is often utilized to generate impedance profiles. The outcome of these algorithms can hence be guaranteed to result in stable control.

In practice, the impedance parameter that has the most significant impact on task performance is the stiffness. Hence, it is often reasonable to give priority to the stiffness design. The damping can then be chosen to guarantee that the desired stiffness profile can be stably executed, typically by using critical damping. Inspection of the constraints of Theorem 1 reveals that the least conservative constraints are given by α chosen so the largest eigenvalue of $\alpha\mathbf{H} - \mathbf{D}(t)$ remains negative during the task. Hence, to have the least conservative constraints, α should be chosen as

$$\alpha = \min_t \frac{\underline{\lambda}(\mathbf{D}(t))}{\overline{\lambda}(\mathbf{H})} \tag{11}$$

where $\overline{\lambda}(.)$ and $\underline{\lambda}(.)$ denote the largest and smallest eigenvalue, respectively. With this choice, the first condition of Theorem 1 is by construction satisfied for all t, as will be demonstrated next. Hence, what remains to be verified is the second condition of Theorem 1. A simple verification procedure is as follows.

1) Given some ideal desired $\mathbf{D}(t)$ and $\mathbf{H}$, determine α according to (11).
2) Verify that $\dot{\mathbf{K}}(t) + \alpha\dot{\mathbf{D}}(t) - 2\alpha\mathbf{K}(t)$ is negative semidefinite for all $t > 0$.
3) If not verified, modify stiffness and/or damping profile.[3]

Below, we show how the constraints in Theorem 1 relate to the eigenvalues of the matrices in the general case. Consider $\mathbf{A} = -\mathbf{D} + \alpha\mathbf{H}$. This matrix needs to be negative definite for negative definiteness of $\dot{V}_2$. $\mathbf{H}$ and $\mathbf{D}$ are symmetric, which implies $\mathbf{A}$ is symmetric and its negative definiteness is hence equivalent all its eigenvalues being negative. In particular, its largest eigenvalue $\overline{\lambda}(\mathbf{A})$ should be negative

$$\overline{\lambda}(\mathbf{A}) = \sup_{\|v\|=1} \mathbf{v}^T\mathbf{A}\mathbf{v} \leq \underbrace{\sup_{\|v\|=1} \mathbf{v}^T(-\mathbf{D})\mathbf{v}}_{=\overline{\lambda}(-D)} + \underbrace{\sup_{\|v\|=1} \mathbf{v}^T(\alpha\mathbf{H})\mathbf{v}}_{\alpha\overline{\lambda}(H)}. \tag{12}$$

Above, the triangle inequality for the supremum norm has been used. Thus, we have

$$\overline{\lambda}(\mathbf{A}) \leq -\underline{\lambda}(\mathbf{D}) + \alpha\overline{\lambda}(\mathbf{H}) \tag{13}$$

since $\overline{\lambda}(-\mathbf{D}) = -\underline{\lambda}(\mathbf{D})$. Consequently, we have that negative definiteness of $\mathbf{A}$ is implied by the following bound on the smallest eigenvalue of $\mathbf{D}$:

$$\underline{\lambda}(\mathbf{D}) > \alpha\overline{\lambda}(\mathbf{H}). \tag{14}$$

Hence, α defines a lower bound for the minimum eigenvalue of $\mathbf{D}$ as a multiple of the maximum eigenvalue of $\mathbf{H}$.

[3]For example, increase constant damping or increase the damping ratio for the common case that the damping is varying with the stiffness to ensure a constant damping ratio.

Now consider the second condition, which bounds the rate of change in stiffness. The following matrix should be negative definite:

$$\mathbf{C} = \dot{\mathbf{K}} + \alpha\dot{\mathbf{D}} - 2\alpha\mathbf{K}. \tag{15}$$

As above, we use the triangle inequality to bound the largest eigenvalue of $\mathbf{C}$:

$$\overline{\lambda}(\mathbf{C}) \leq \overline{\lambda}(\dot{\mathbf{K}}) + \alpha\overline{\lambda}(\dot{\mathbf{D}}) - 2\alpha\underline{\lambda}(\mathbf{K}). \tag{16}$$

It follows that a sufficient condition for negative definiteness of $\mathbf{C}$ is given by

$$\overline{\lambda}(\dot{\mathbf{K}}) < 2\alpha\underline{\lambda}(\mathbf{K}) - \alpha\overline{\lambda}(\dot{\mathbf{D}}). \tag{17}$$

IV. Evaluation

A. Simulations

To illustrate the properties of the proposed approach, we present a set of simulations comparing the stability analysis tools from Section III with the recently proposed tank-based approach to varying stiffness control [8]. As in real interaction control scenarios, the goal is not accurate trajectory following, but accurate implementation of the desired interactive behavior. In these scenarios, the latter is defined by a time-dependent stiffness profile, and the goal is hence to follow this as accurately as possible while ensuring stability.

1) Tracking Task: First we shall consider an example of 1 degree of freedom (dof) system that is unstable due to a varying stiffness profile. This is a reproduction of the simulation in [8]. The reference trajectory and the desired stiffness profile are given by

$$x_t^d = 10\sin(0.1t) \tag{18a}$$

$$k_t^d = k_0 + 10\sin(0.1t) \tag{18b}$$

with $k_0 = 12$. The system is simulated with a mass of 10 Kg and a damping of 1 Ns/m. Fig. 2(a) shows a simulation of 100 s of this system under standard impedance control. As can be seen in the energy plot in Fig. 2(a), V_1 as well as V_2 are nonmonotonic and with increasing magnitude. Note that in this simulation, which is a linear scalar system with varying stiffness, there are no other factors contributing to the observed unstable behavior. Since the system is unstable, our method cannot validate it. As described in Section III-B, this should be tackled by modifying the impedance profile such that it passes the validation. Simply changing the constant stiffness component as $k_0 = 18$ is sufficient for the impedance profile to be validated. This is shown in Fig. 2(b), which plots the stiffness profile and evolution of the energy function V_2, (21), during a 10 s simulation. When doing the same simulation with the controller from [8], the stiffness profile has to be modified online, as can be seen in Fig. 2(c). The discontinuities in the stiffness profile are a result of the formulation in [8], which will fall back to a predefined constant component of stiffness when the tank is empty. When and to what extent this effect occurs depends on the choice of the open tank parameters and more importantly the state of the robot as the stiffness variations take place.

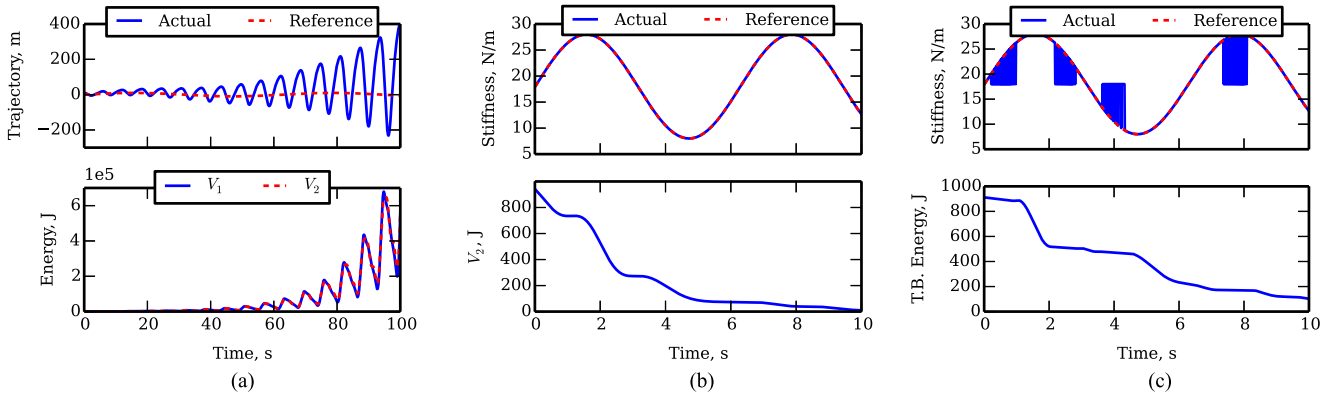

Fig. 2. (a) Trajectory and the Lyapunov candidates V_1 and V_2 (5 and 21) during a simulation of a single dof with mass 10 Kg, damping 1 Ns/m and desired trajectory and stiffness given by (18) with $k_0 = 12$. (b) Stiffness and V_2, (21), during standard impedance control with $k_0 = 18$ and stability validated according to procedure in Section III-B. (c) Stiffness and energy function from the tank-based method [8], with modified stiffness profile, $k_0 = 18$.

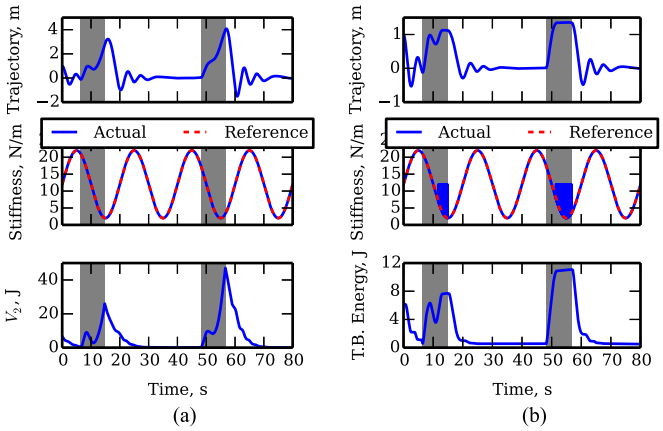

Fig. 3. (a) Trajectory, stiffness, and evolution of V_2. The data come from a 80 s simulation of a regulation task. The system is perturbed by the application of a constant force during the shaded areas. Here, the standard impedance controller is used since the desired stiffness profile is guaranteed to be stable. This fact is confirmed here by the monotonic decrease of V_2 outside the shaded regions. (b) Same as (a) but system controlled with tank-based approach from [8]. The bottom plot shows the time series of the tank-based energy function. Note that it is in particular during perturbations that the system is unable to use the desired stiffness.

2) Regulation With Perturbations: The advantage of ensuring stability of a varying impedance profile without dependency on state measurements is most clear in situations where perturbations are to be expected during task executions and a reliable trajectory prediction is not possible. By inspection of (6), it is clear that it is particularly in the presence of a large position error $\tilde{\mathbf{q}}$ that energy is injected into the system if the stiffness is increased. Online methods such as [8] are sensitive to perturbations during the task whereas our method is not. To illustrate this, we simulated a one dof regulation task with a varying stiffness profile given by

$$k = 12 + 10 \sin\left(\frac{\pi}{10} t\right) \tag{19}$$

and a constant damping 4 Ns/m and a mass of 10 Kg. Fig. 3(a) shows that the impedance profile is validated by Theorem 1 and the trajectory resulting from the simulation. A constant, positive perturbation force was applied in intervals shaded gray in the plots. Fig. 3(b) shows the results of the tank-based method. Note that it is in particular when the system is perturbed that the tank controller has to fall back to the constant stiffness value. We wish to emphasize that this is not a problem particularly related to the tank-based stabilization method, but rather a general problem of any stabilization method relying on state measurements during task execution.

B. Validation of Real Impedance Profiles

Although it has been shown that varying stiffness can lead to unstable behavior, experience shows that this is a rare occurrence in practice. There already esixts several works that have used varying stiffness controllers which have not resulted in unstable behavior. However, stability has only been proven in special cases where the stiffness is varied according to an adaptive control law such as [29] or with a particular parametric model as in our previous work [15]. For the more general case, where the stiffness can be considered a time-varying function just like the trajectory, Theorem 1 can be used to validate or reject stiffness profiles. Since our stability condition is conservative,[4] it is important to investigate if in practice it can be used to validate stiffness trajectories. Therefore, we gathered data from three previous works by ourselves and others, and tested to see if our stability condition could validate these impedance profiles. In each case, a control scheme with inverse dynamics and damping varying as a function of the stiffness (so as to maintain a critically damped system) was assumed. First, for each case, a value of α was selected according to (11). Then, the following time-varying matrix was computed:

$$\dot{\mathbf{K}}(t) + \alpha \dot{\mathbf{D}}(t) - 2\alpha \mathbf{K}(t). \tag{20}$$

The stability according to Theorem 1 is then confirmed if all eigenvalues of (20) remain negative.

The first dataset is a match-lighting task from our previous work [19]. This experiment was carried out on the 7-dof KUKA LWR 4+ robot arm, see Fig. 4. A joint stiffness profile was taught to the robot using a physical human–robot interface designed

[4] In the sense that there are stable impedance profiles that do not satisfy Theorem 1.

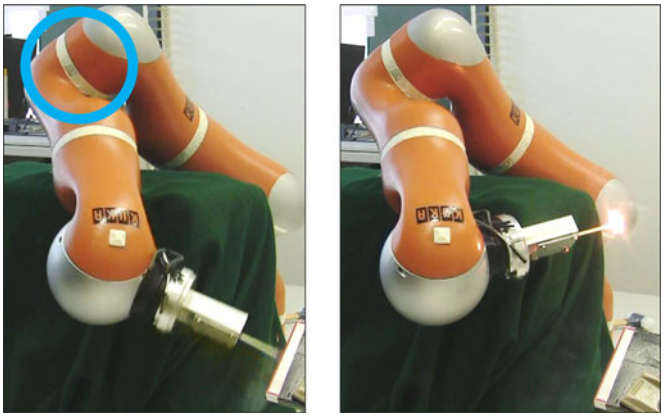

Fig. 4. Figure shows snapshots from the match-lighting task using varying joint stiffness.

for this purpose. The resulting stiffness profile is a constant, high stiffness for all joints except the elbow joint (encircled in Fig. 4), in which the stiffness is reduced as the robot strikes the match on the matchbox. The stiffness profile for the elbow joint is shown in Fig. 5(a), top. Fig. 5(b), bottom shows the evolution of the largest eigenvalue of (20). Note that only one of the eigenvalues are plotted since the other six remain constant throughout the task.

The second dataset comes from Calinon *et al.* [6]. The task is a two-dimensional reaching task where the final part of the trajectory passes through a narrow path leading to the target. The trajectory and varying stiffness are generated online by Gaussian mixture regression (GMR) and minimum intervention control scheme using the covariance from GMR to find a stiffness profile. Fig. 5(b) shows the eigenvalues of the stiffness matrix and (20). As can be seen, both eigenvalues remain negative throughout the time series and the impedance profile is hence validated as stable.

The third dataset comes from Buchli *et al.* [4], who applied the reinforcement learning algorithm PI2 to simultaneously learn the trajectory and stiffness profile repeated task trials evaluated by a given cost function. The task is a via-point task in a 6d joint space implemented on a KUKA LWR robot (the last joint was ignored). The cost function was designed to favor a compliant behavior when accuracy is not needed. This resulted in a stiffness profile with a low stiffness that locally increases when the robot passes near the via point. Fig. 5(c) shows the time series of the eigenvalues of the stiffness matrix and (20), respectively. As in the previous examples, all eigenvalues clearly remain negative.

V. Discussion

The most fundamental property that should be required from a control system is stability. This is especially important in applications of robots near humans, in which variable impedance control is particularly interesting to use. While experience tells us that unstable behavior arising from variable impedance is quite rare in practice, it is important to better understand this issue and it is crucial to subject the impedance variations to constraints so that stability is guaranteed. In this paper, we proposed a novel, state-independent stability condition for varying stiffness and damping profiles.

Impedance control is commonly used in situations where significant departure from the reference trajectory can be expected by either temporary perturbations or physical constraints in the environment. For this reason, the reference trajectory is often renamed virtual trajectory in impedance control literature, highlighting the fact that perfect tracking of the reference may not be possible or even desired. As shown by the simulation in Section IV-A.2, using the classical Lyapunov function as a stability observer will make it difficult to modify the stiffness in the presence of significant position errors. The method proposed in this paper does not have this limitation since it is independent of state measurements during task execution (see Section III). Our methodology involves selecting the parameter α in Theorem 1. There may be many different values of α that can be used to validate a stable impedance profile. Conversely, a poorly chosen α can lead to overly conservative constraints that disqualify an impedance profile that would have been validated by another choice of α. To facilitate this choice, we described in Section III-B a systematic method of choosing α and making changes to the impedance profile so that the system can be validated.

The main limitation of the proposed approach is that it requires the inertia matrix H to be constant. This in turn requires model knowledge and dynamic decoupling (requiring measurement of external effort in interaction task) as described in Section II-B. This limitation may be more problematic in the Cartesian case, where it may be impossible to keep H constant near singular configurations. Impedance control can be implemented with simplified controls, requiring only a gravity model and no measurement of external force/torque [11]. For this case, our method is not applicable since the apparent inertia becomes equal to the natural inertia of the robot which is configuration dependent. The state-dependent tank-based method proposed in [8] does not have this limitation.

It is possible to construct variable impedance profiles that yield qualitatively stable behavior but that are not validated by Theorem 1. This is because Theorem 1 is a conservative guarantee of stability. Our experience is that it will validate reasonably chosen impedance profiles, as shown in Section IV-B. Depending on how the task and on the particular controller and chosen parameters, state-dependent alternatives such as [8] may be more or less conservative than the approach presented in this paper. Hence, it is not possible to make any general conclusions about which approach is less conservative. It should be mentioned however, that the tank-based method [8] and other methods depending on open parameters need to be tuned for each task that they are applied to. Our method has no open parameters but can still validate reasonable impedance profiles. Which method is to be used ultimately depends on factors such as importance of accurate stiffness following (choose our approach) or applicability to systems without dynamic decoupling (choose state-dependent approach such as [8]).

Appendix A
Lyapunov Theorem for Nonautonomous Systems

A nonlinear, nonautonomous system $\dot{\xi} = f(\xi, t)$ is uniformly Lyapunov-stable at the origin if there exists a scalar function $V(\xi, t)$, such that

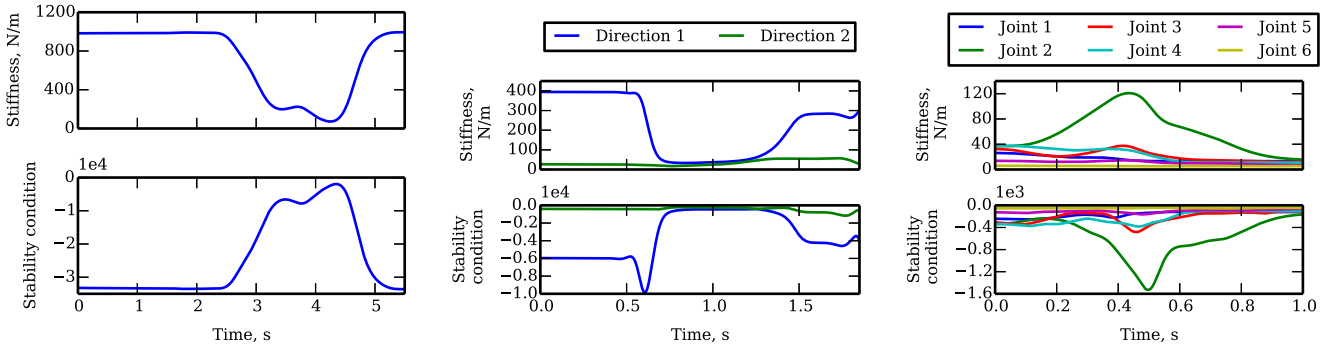

Fig. 5. (a) Varying stiffness profile and (20) for data from match-lighting task in [19]. (b) Stiffness eigenvalues over time and the evolution of the eigenvalues of (20) for data from [6]. The eigenvalues remain negative definite and the impedance profile is hence guaranteed to yield stable control. (c) The joint stiffness profile and corresponding eigenvalues of (20) for a 6-dof joint space via point task with varying stiffness. This data come from [4].

1) positive definiteness of V:

$$V(\xi,t) > 0 \;\; \forall \xi \neq \mathbf{0}, \; \forall t \geq 0, \quad \text{and } V(\mathbf{0},t) = 0, \; \forall t \geq 0$$

2) negative semidefiniteness of $\dot{V}$:

$$\dot{V}(\xi,t) \leq 0, \forall \xi \neq \mathbf{0}, \; \forall t \geq 0, \quad \text{and } \dot{V}(\mathbf{0},t) = 0, \; \forall t \geq 0$$

3) decrescense of V:

$$\exists \quad V'(\xi) > 0, \forall \xi \neq \mathbf{0} : \quad V(\xi,t) \leq V'(\xi), \; \forall t \geq 0.$$

It is globally uniformly asymptotically stable if in addition:

1) negative definiteness of $\dot{V}$:

$$\dot{V}(\xi,t) < 0, \forall \xi \neq \mathbf{0}, \; \forall t \geq 0, \quad \text{and } \dot{V}(\mathbf{0},t) = 0, \; \forall t \geq 0$$

2) radial unboundedness of V in ξ:

$$\|\xi\| \to \infty \Rightarrow V(\xi,t) \to \infty.$$

APPENDIX B
PROOF OF THEOREM 1

Consider the following Lyapunov candidate function:

$$V_2(\tilde{\mathbf{q}}, \dot{\tilde{\mathbf{q}}}, t) = \frac{(\dot{\tilde{\mathbf{q}}} + \alpha\tilde{\mathbf{q}})^T \mathbf{H} (\dot{\tilde{\mathbf{q}}} + \alpha\tilde{\mathbf{q}})}{2} + \frac{\tilde{\mathbf{q}}^T \boldsymbol{\beta}(t) \tilde{\mathbf{q}}}{2} \tag{21}$$

where $\boldsymbol{\beta}(t)$ is a symmetric, positive semidefinite, and continuously differentiable matrix. Differentiating yields

$$\dot{V}_2(\tilde{\mathbf{q}}, \dot{\tilde{\mathbf{q}}}, t) = (\dot{\tilde{\mathbf{q}}} + \alpha\tilde{\mathbf{q}})^T \mathbf{H} (\ddot{\tilde{\mathbf{q}}} + \alpha\dot{\tilde{\mathbf{q}}}) + \tilde{\mathbf{q}}^T \boldsymbol{\beta}(t) \dot{\tilde{\mathbf{q}}} + \frac{1}{2} \tilde{\mathbf{q}}^T \dot{\boldsymbol{\beta}}(t) \tilde{\mathbf{q}}. \tag{22}$$

Substituting the closed-loop dynamics from (2) with $\tau_e = \mathbf{0}$ and rearranging yields

$$\begin{aligned} \dot{V}_2(\tilde{\mathbf{q}}, \dot{\tilde{\mathbf{q}}}, t) = {} & \dot{\tilde{\mathbf{q}}}^T \{\alpha\mathbf{H} - \mathbf{D}(t)\} \dot{\tilde{\mathbf{q}}} \\ & + \dot{\tilde{\mathbf{q}}}^T \left\{\boldsymbol{\beta}(t) + \alpha^2\mathbf{H} - \mathbf{K}(t) - \alpha\mathbf{D}(t)\right\} \tilde{\mathbf{q}} \\ & + \tilde{\mathbf{q}}^T \left\{\frac{1}{2}\dot{\boldsymbol{\beta}}(t) - \alpha\mathbf{K}(t)\right\} \tilde{\mathbf{q}}. \end{aligned} \tag{23}$$

In order to eliminate the cross term between $\tilde{\mathbf{q}}$ and $\dot{\tilde{\mathbf{q}}}$, define $\boldsymbol{\beta}(t)$ as

$$\boldsymbol{\beta}(t) = \mathbf{K}(t) + \alpha\mathbf{D}(t) - \alpha^2\mathbf{H} \quad \Rightarrow \quad \dot{\boldsymbol{\beta}}(t) = \dot{\mathbf{K}}(t) + \alpha\dot{\mathbf{D}}(t). \tag{24}$$

Substituting $\boldsymbol{\beta}(t)$ and $\dot{\boldsymbol{\beta}}(t)$ into (23) then yields

$$\begin{aligned} \dot{V}_2(\tilde{\mathbf{q}}, \dot{\tilde{\mathbf{q}}}, t) = {} & \dot{\tilde{\mathbf{q}}}^T \{\alpha\mathbf{H} - \mathbf{D}(t)\} \dot{\tilde{\mathbf{q}}} \\ & + \tilde{\mathbf{q}}^T \left\{\frac{1}{2}\dot{\mathbf{K}}(t) + \frac{\alpha}{2}\dot{\mathbf{D}}(t) - \alpha\mathbf{K}(t)\right\} \tilde{\mathbf{q}}. \end{aligned} \tag{25}$$

Note that $\boldsymbol{\beta}(t)$ is positive semidefinite [substitute condition 1 from Theorem 1 in (24)], which implies that V_2 is also positive semi-definite. V_2 is also decrescent, since it is dominated, e.g., by $V_2(\tilde{\mathbf{q}}, \dot{\tilde{\mathbf{q}}}, t) =< (\dot{\tilde{\mathbf{q}}} + \alpha\tilde{\mathbf{q}})^T \mathbf{H} (\dot{\tilde{\mathbf{q}}} + \alpha\tilde{\mathbf{q}}) + \|\tilde{\mathbf{q}}\|^2 \max_t \overline{\lambda}(\boldsymbol{\beta}(t))$. Furthermore, V_2 is radially unbounded, and substituting condition 2 from Theorem 1 in (25) confirms $V_2 \leq 0$ for all $\tilde{\mathbf{q}}, \dot{\tilde{\mathbf{q}}} \neq \mathbf{0}$, which concludes the proof. Replacing semidefiniteness in conditions of Theorem 1 with positive definiteness analogously yields a $V_2 < 0$ for all $\tilde{\mathbf{q}}, \dot{\tilde{\mathbf{q}}} \neq \mathbf{0}$, proving asymptotic stability in that case.

REFERENCES

[1] A. Ajoudani, N. Tsagarakis, and A. Bicchi, "Tele-impedance: Teleoperation with impedance regulation using a body-machine interface," *Int. J. Robot. Res.*, vol. 31, no. 13, pp. 1642–1656, Oct. 2012.

[2] A. Bicchi, G. Tonietti, M. Bavaro, and M. Piccigallo, "Variable stiffness actuators for fast and safe motion control," in *Proc. 11th Int. Symp. Robot. Res.*, 2005, vol. 15, pp. 527–536.

[3] D. Braun, M. Howard, and S. Vijayakumar, "Optimal variable stiffness control: Formulation and application to explosive movement tasks," *Auton. Robots*, vol. 1, no. 17, pp. 237–253, 2012.

[4] J. Buchli, F. Stulp, E. Theodorou, and S. Schaal, "Learning variable impedance control," *Int. J. Robot. Res.*, vol. 30, no. 7, pp. 820–833, 2011.

[5] S. Calinon, I. Sardellitti, and D. Caldwell, "Learning-based control strategy for safe human-robot interaction exploiting task and robot redundancies," in *Proc. IEEE/RSJ Int. Conf. Intell. Robots Syst.*, 2010, pp. 249–254.

[6] S. Calinon, D. Bruno, and D. G. Caldwell, "A task-parameterized probabilistic model with minimal intervention control," in *Proc. IEEE Int. Conf. Robot. Autom.*, May 2014, pp. 3339–3344.

[7] E. Colgate and N. Hogan, "Robust control of dynamically interacting systems," *Int. J. Control*, vol. 48, no. 1,pp. 65–88, 1988.

[8] F. Ferraguti, C. Secchi, and C. Fantuzzi, "A tank-based approach to impedance control with variable stiffness," in *Proc. IEEE Int. Conf. Robot. Autom.*, May 2013, pp. 4948–4953.

[9] M. Garabini, A. Passaglia, F. Belo, P. Salaris, and A. Bicchi, "Optimality principles in stiffness control: The VSA hammer," in *Proc. IEEE/RSJ Int. Conf. Intell. Robots Syst.*, 2011, pp. 3770–3775.

[10] R. Ham, T. Sugar, B. Vanderborght, K. Hollander, and D. Lefeber, "Compliant actuator designs," *IEEE Robot. Autom. Mag.*, vol. 16, no. 3, pp. 81–94, Sep. 2009.

[11] N. Hogan, "Impedance control: An approach to manipulation," *J. Dyn. Syst. Meas. Control*, vol. 107, no. 12, pp. 1–24, 1985.
[12] N. Hogan, "On the stability of manipulators performing contact tasks," *IEEE J. Robot. Autom.*, vol. 4, no. 6, pp. 677–686, Dec. 1988.
[13] M. Howard, D. J. Braun, and S. Vijayakumar, "Transferring human impedance behavior to heterogeneous variable impedance actuators," *IEEE Trans. Robot.*, vol. 29, no. 4, pp. 847–862, Aug. 2013.
[14] S. Jung, T. C. Hsia, and R. G. Bonitz, "Force tracking impedance control of robot manipulators under unknown environment," *IEEE Trans. Control Syst. Technol.*, vol. 12, no. 3, pp. 474–483, May 2004.
[15] M. Khansari-Zadeh, K. Kronander, and A. Billard, "Modeling robot discrete movements with state-varying stiffness and damping: A framework for integrated motion generation and impedance control," in *Proc. Robot. Sci. Syst.*, 2014.
[16] O. Khatib, "A unified approach for motion and force control of robot manipulators: The operational space formulation," *IEEE J. Robot. Autom.*, vol. 3, no. 1, pp. 43–53, Feb. 1987.
[17] P. Kormushev, S. Calinon, and D. Caldwell, "Robot motor skill coordination with EM-based reinforcement learning," in *Proc. IEEE/RSJ Int. Conf. Intell. Robots Syst.*, 2010, pp. 3232–3237.
[18] K. Kronander and A. Billard, "Online learning of varying stiffness through physical human-robot interaction," in *Proc. IEEE Intl Conf. Robot. Autom.*, 2012.
[19] K. Kronander and A. Billard, "Learning compliant manipulation through kinesthetic and tactile human-robot interaction," *Trans. Haptics*, vol. 7, no. 3, 2013, pp. 1–16.
[20] T. Lozano-Perez, M. T. Mason, and R. H. Taylor, "Automatic synthesis of fine-motion strategies for robots," in *Proc. Int. J. Robot. Res.*, 1984, pp. 3–24.
[21] J. Medina, D. Sieber, and S. Hirche, "Risk-sensitive interaction control in uncertain manipulation tasks," in *Proc. IEEE Int. Conf. Robot. Autom.*, 2013.
[22] G. Palli, C. Melchiorri, and A. D. Luca, "On the feedback linearization of robots with variable joint stiffness," in *Proc. IEEE Int. Conf. Robot. Autom.*, 2008, pp. 1753–1759.
[23] E. Rombokas, M. Malhotra, E. Theodorou, E. Todorov, and Y. Matsuoka, "Tendon-driven variable impedance control using reinforcement learning," in *Proc. Robot. Sci. Syst.*, 2012.
[24] W. J. Rugh and J. S. Shamma, "Research on gain scheduling," *Automatica*, vol. 36, pp. 1401–1425, 2000.
[25] J. S. Shamma and M. Athans, "Gain scheduling: Potential hazards and possible remedies," *IEEE Control Syst.*, vol. 12, no. 3, pp. 101–107, Jun. 1992.
[26] J.-J. Slotine and W. Li, *Applied Nonlinear Control*. Englewood Cliffs, NJ, USA: Prentice Hall, 1991.
[27] J.-J. E. Slotine, "On the adaptive control of robot manipulators," *Int. J. Robot. Res.*, vol. 6, pp. 49–59, 1987.
[28] L. Villani and J. De Schutter, "Force control," in *Handbook of Robotics*. New York, NY, USA: Springer, Jul. 2008.
[29] C. Yang, G. Ganesh, S. Haddadin, S. Parusel, A. Albu-Schaffer, and E. Burdet, "Human-like adaptation of force and impedance in stable and unstable interactions," *IEEE Trans. Robot.*, vol. 27, no. 5,pp. 918–930, Oct. 2011.